Overview and application of FEM methods for shock analysis in space instruments

Andrés García-Pérez[a,*], Félix Sorribes-Palmer[a,1], Gustavo Alonso[a], Ali Ravanbakhsh[b]

[a] Instituto Universitario de Microgravedad "Ignacio Da Riva" (IDR/UPM), Universidad Politécnica de Madrid, Pza. Cardenal Cisneros 3, 28040 Madrid, Spain

[b] Institute of Experimental and Applied Physics, Christian-Albrechts-Universität zu Kiel (IEAP-CAU), D-24118, Kiel, Germany

[*]Corresponding author: andres.garcia.perez@upm.es
felix.sorribespalmer@v2c2.at
gustavo.alonso@upm.es
ravanbakhsh@physik.uni-kiel.de

Abstract
Spacecraft are subjected to severe mechanical loads, especially during the ascent phase of the launch. Among several vibrational environments, shock loads, which are caused mainly by the activation of pyrotechnic devices used for the separation of the payloads and the different stages of the launcher, are transmitted throughout the entire structure and reach the scientific instruments of the spacecraft. Therefore, it is important to verify if the space instruments can withstand this environment, considering the nature of the shock, which generally consists in an intensive and short load. In recent years, the demand of numerical analyses to predict the responses of the structures against shocks is increasing and, for this reason, it is necessary to establish adequate numerical methods, taking into account the complex mathematical treatment and the uncertainty in the load characterization. The purpose of this paper is to present the application of different methods to calculate the required structural results for a space instrument subjected to the shock environments using a finite element model (FEM). The procedures for each method, the type of the results that can be calculated and the comparison of the results are described in this paper. The objective is to select the most suitable analysis method for shock loads based on the precision of the results and the capability of obtaining all the variety of data for a complete evaluation of the structure.

Keywords: shock, space instrument, finite element model, structural verification, transient analysis, response spectrum analysis

1 Introduction

A mechanical environment that combines high static acceleration, low and high frequencies vibrations and shock loads, is generated during the launch operation in space missions. These loads are transmitted to the equipment and components of the spacecraft through the mechanical interfaces. Hence, the structural verification of spacecraft and their instruments is a fundamental

[1]Graz University of Technology, Inffeldgasse 21 / A, 8010 Graz, Austria

requirement, where each type of the mechanical loads must be simulated by test and analysis to qualify the mechanical design [1,2].

When a shock load is propagated throughout the entire structure, it generates tension-compression, flexural and shear waves which are reflected, dissipated and diffracted at mechanical interfaces. The response acceleration has a transient and oscillatory behavior, with high positive and negative peaks, which is rapidly decreased with the time. In terms of frequency, the shock response is composed mainly by the system natural frequencies (typically at lower frequency) and by the frequencies from the external loading, usually at high frequency.

The shock environment is divided into the following categories depending on the distance of the measured point or the analyzed part with respect to the shock source [3,4]:

- The near-field shock environment occurs when the analyzed structure is near the shock source. The signal presents very high acceleration peaks (more than 5000 g) and very high frequency content (it can reach 1 MHz), due to that the wave is dominated by direct wave propagation.
- The mid-field shock environment is characterized by a combination of direct propagation and structure resonances, which generates a signal with high peaks between near and far-field shocks and frequency content until 100 kHz.
- The far-field shock environment appears to a distance far enough from the shock source, where the wave is dominated by the structural modal behavior. The response signals present high peaks but lower than from near and mid fields environments and with a frequency content not higher than 10 kHz.

Each launch authority must specify the shock loads generated by its launch vehicle during its operation taking into account all of the different causes. Due to the difficulty to elaborate a shock specification by transient acceleration functions, the adopted criterion in space industry is to represent the shock environment by a SRS curve [4]. A time acceleration function can be converted into the corresponding SRS curve by calculating the maximum peak acceleration of the response of a single degree of freedom system (SDOF) when the aforementioned acceleration time function is applied to the base [5]. The SRS curve is built establishing the dependency of the peak value of the response acceleration with the natural frequency of the SDOF, for a constant value of damping (the standard value for shock is 0.05). For space structures subjected to a far-field shock environment, the SRS are composed typically by an initial ramp from 100 Hz to a cut-off frequency (between 1000 and 2000 Hz) in a log-log graph, followed by a section of constant SRS until 10000 Hz [4]. The specification should be accompanied by a description of the expected time signal shape and duration, which typically is oscillatory and with a characteristic duration of 20 ms.

Important information about the shock nature as duration or excitation frequencies is lost when only the SRS curve is considered. In the cases where the shock specification of a space structure consists in a SRS curve, the only available information about the shock is the maximum peak acceleration of the structure simplified as a SDOF excited on its base by an unknown acceleration time function. This fact implies that the structure can be verified considering any transient load which meets with the specified SRS. Therefore, when the definition of an input acceleration time function from the SRS specification is required to test or analyze a satellite or a space instrument, extra information must be added to create the acceleration function. This fact implies that different functions can be used to evaluate the same shock environment. The

input acceleration function can be obtained from several numerical methods as damped sinusoids decomposition, wavelet synthesis [5] or with the modal characteristics of the analyzed structure [6].

There are different ways to simulate shock loads in space systems [3,4] with the aim to verify if these structures can withstand this environment. The most used verification approach is the shock testing [7], which can be done by electromechanical shakers or by the test facilities where the shock is generated by mechanical impacts using hammer pendulums [8-12] or shooting projectiles [13-15].

Nowadays, the demand of numerical analyses to prove the structural reliability with a certain accuracy is increasing due to the difficulty to know from the shock test data the required results such as stresses, forces and accelerations in the critical parts. The state of the art for shock analysis has not reached the level of maturity as for the other loads such as static or sine vibration due to the high frequency content. There are some aspects that hinder the numerical treatment of this type of loads, such as short duration, broad range of excitation frequencies (typically from 100 to 10000 Hz for far-field environment), nonlinearity and the other effects in the propagation of the shock waves like the attenuation caused by distance and discontinuities in bolted interfaces of the structure. For these reasons, different analysis methods have been proposed and studied to calculate the structural behavior resulted from shock loads [16], where the required results as stresses, strains, forces and accelerations are necessary to evaluate the integrity of the space structures.

Finite Element Analysis (FEA), which is the most employed method in space industry for static and dynamic structural analyses, can be adequate to analyze small structures like space instrument subjected to a far-field shock load because its response is mainly dominated by the modal behavior. Nonlinear effects as attenuation due to the distance have less impact on the results for these structures. FEA method has been validated in several aspects simulating shock loads and comparing with the test data. In [17], different modeling techniques for a PCB (detailed FEM with 3D elements and simplified FEM with 2D elements) are studied simulating the shock load by transient analysis getting a good correlation with the test results for both models. In [18] the influence of the parameters that define an input load represented by a trapezoidal force impulse in a FEM transient analysis is studied and correlated with test results. The modeling of joints is evaluated in [19] for a truss frame structure under shock load, and the effects of a new damping definition for bolted joints of space structures is studied in [20]. In [21] the effect of the nonlinear modeling for the clamp band joint is evaluated in a coupling dynamic FEM of a launcher and spacecraft system subjected to vibration and impact excitations, and in [22] the characteristics of the design of the clamp band are studied to evaluate several structural parameters on the attitude of separating satellite, dynamic envelope of clamp band and the separation shock. Other studies employ detailed FEM with 3D elements to have more accurate results of shock analyses [23-27], with the disadvantage of time consuming and the big amount of output data. Alternative numerical approaches to simulate shocks are the Statistical Energy Analysis (SEA) method, which can be combined with FEA [28] or with Virtual Mode Synthesis and Simulation (VMSS) [29], Spectral Element Method (SEM) [30] and hydrocodes [27]. The advantage of FEA approach compared to the other numerical approaches is that it is a widely used method in the space industry for static, sine vibration and random vibration structural analyses and can also be easily implemented for shock analysis using the same FEM or with few modifications. FEA approach provides an acceptable prediction for small structures, where

it is less problematic to have a sufficiently fine mesh without an excessive quantity of nodes to achieve the appropriate accuracy for the shock simulations.

The purpose of this paper is to present a complete overview of the different methods of shock analysis using the finite element model of a space instrument, indicating the characteristics and the results that can be calculated for each analysis. The simulation results are compared to the shock test data to determine the precision of each analysis method. One of the main conclusions of the work is that despite the required computational time comparing with the rest of the methods, the modal transient analysis is the most complete and accurate of the studied methods, getting an acceptable prediction of the structural behavior of the instrument under the shock environment.

2 STEP instrument for Solar Orbiter spacecraft

The Supra Thermal Electrons and Protons (STEP) instrument constitutes together with other instruments (the Electron Proton Telescope – High Energy Telescope (EPT-HET) instrument, the Suprathermal Ion Spectrograph (SIS) and the Instrument Control Unit (ICO)) the Energetic Particle Detector (EPD) payload for the ESA-NASA Solar Orbiter spacecraft, which is scheduled to be launched in 2019. The main objective of the Solar Orbiter project is to obtain a better understanding of the heliosphere characteristics.

The STEP instrument (Figure 2-1) has been designed by a research team at the Institute of Experimental and Applied Physics (IEAP) of the Christian Albrechts University of Kiel (CAU) in Germany. STEP consists of two detectors of low energy electrons and protons (in the range of 3keV to 100keV). Both detectors are mounted on an electronic box, and two radiators are included to evacuate the excess of heat in the instrument. Further details about the scientific objectives of STEP instrument as well as Solar Orbiter EPD can be found in [31].

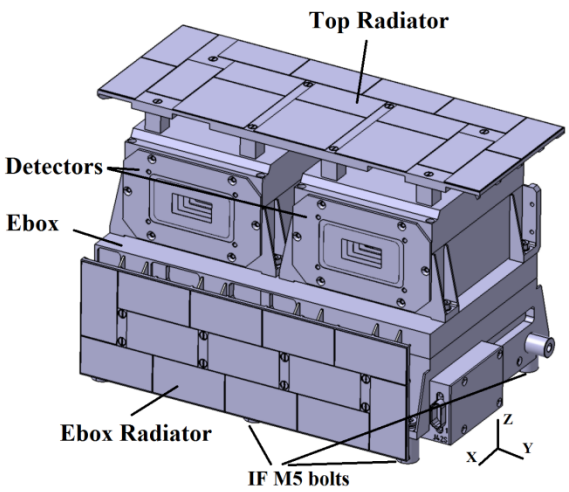

Figure 2-1: CAD design of STEP instrument

The total mass of the instrument is 2 kg approximately, and its maximum dimensions are 127 x 188 x 137 mm. The mechanical interface is constituted by 6 M5 bolts, which attach the instrument to the spacecraft panel via a mounting bracket. The mechanical loads as shock and vibrations produced during the launch phase will be transmitted to the instrument through these 6 interface joints.

The shock verification approach for STEP combines the shock tests data and FEM analysis to evaluate the possible damage of the sensitive parts due to high acceleration levels of shock loads.

2.1 Shock tests of STEP instrument

The shock tests of the instrument were performed at the Airbus Defence & Space Environmental Testing Laboratories in Portsmouth, England. The test method consists in using a horizontal drop table hosting the instrument and its adaptor plate (Figure 2-2). The table is hit by a mass to simulate the shock environment in each of the orthogonal axes of the instrument. The mass, drop height and contact material at the hitting point are chosen to generate a shock load as close as possible to the corresponding SRS specification. In addition, a dummy mass representing STEP is used to calibrate the shock signal prior to actual testing on the STEP instrument.

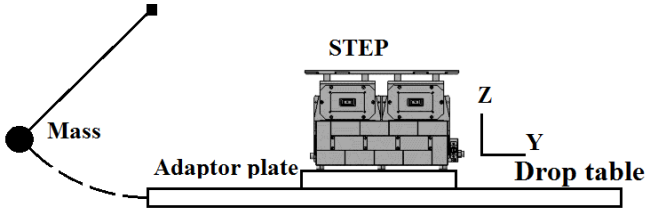

Figure 2-2: Shock test setup in Y direction

To measure the input acceleration, two reference triaxial accelerometers are located on the unit adaptor plate fixed to the shock table near to two diagonally opposite interface bolts (Figure 2-3a). Both accelerometers obtain the input signal in each of the three orthogonal axes, allowing to know if the shock test generates non-negligible accelerations in the directions perpendicular to the intended excitation axis.

A set of accelerometers (6 triaxial and 3 unidirectional) are located in different positions of the instrument to measure its response to shock loads (Figure 2-3). With these accelerometers, the time acceleration functions and their corresponding SRS curves are experimentally obtained and are used in this study for the comparison with the simulation results.

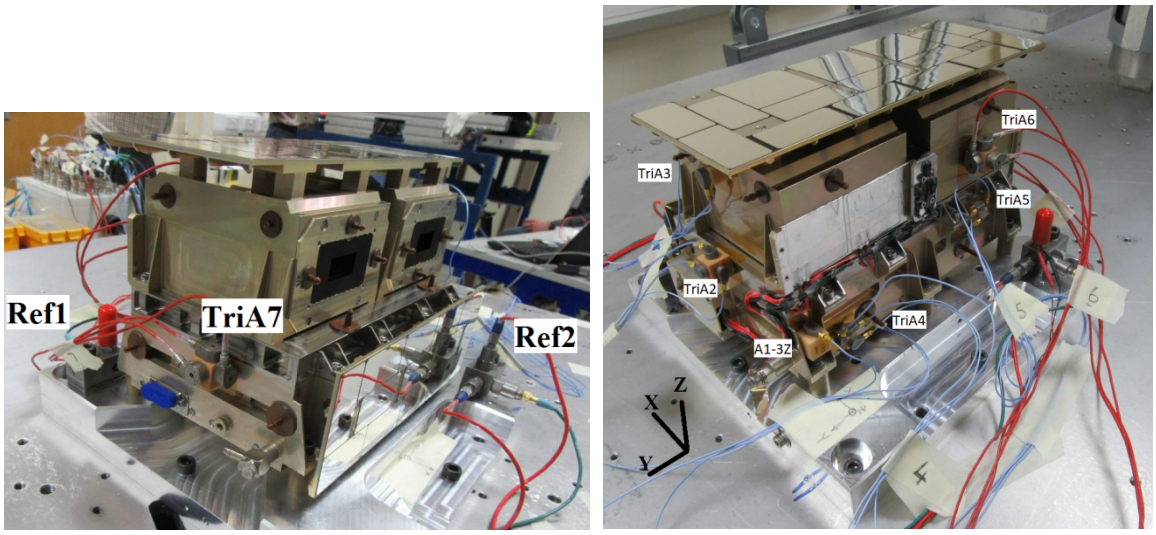

a) b)

Figure 2-3: Reference accelerometers (Ref1 and Ref2), triaxial response accelerometers (TriA2, TriA3, TriA4, TriA5, TriA6 and TriA7) and unidirectional accelerometer (A1-3Z) location in the STEP instrument for shock test

The shock test considered in this study is the qualification shock in the instrument Y direction (Figure 2-2). The test input SRS curves in Y axis meet the requirement of being between the low limit (-3 dB) and the high limit (+6 dB) with respect to the SRS specification (Figure 2-4). As can be seen in Figure 2-5, Figure 2-6 and Figure 2-7, the differences of the signals measured by both reference accelerometers are small and the levels of the cross acceleration in Z axis are on the order of magnitude of the levels in the main direction (Y axis).

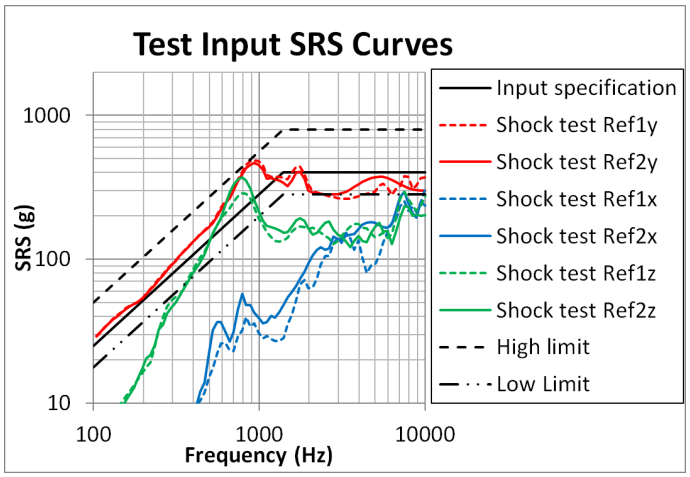

Figure 2-4: Input SRS curves of the shock test in Y direction measured by Ref1 and Ref2 accelerometers

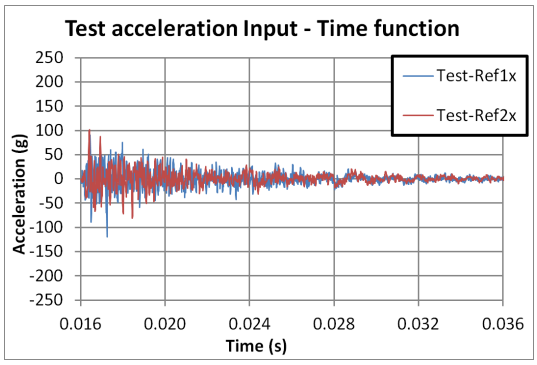

Figure 2-5: Input time signals for shock test measured by Ref1 and Ref2 accelerometers in X direction

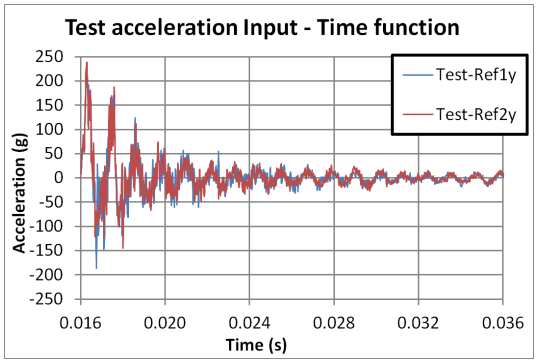

Figure 2-6: Input time signals for shock test measured by Ref1 and Ref2 accelerometers in Y direction

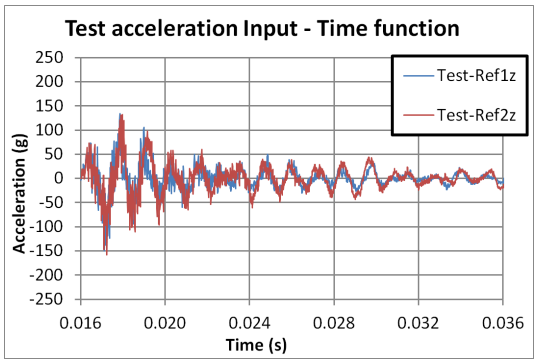

Figure 2-7: Input time signals for shock test measured by Ref1 and Ref2 accelerometers in Z direction

2.2 FEM description

The recommended method for structural calculation in European space projects is the Finite Element Analysis (FEA) and, for the European project of Solar Orbiter, the use of Nastran code for the FEM structural analyses is a requirement. The initial objective of the FEM of STEP instrument (Figure 2-8) is the calculation of the main results (stresses, strains, forces) for the standard structural load cases such as static with inertial loads, sine vibration and random vibration. The model is constituted by 79537 nodes and 79849 elements, mainly 2D shell quadrilateral (QUAD4) and triangular (TRIA3) elements. The triangular elements are distributed in geometrically complex zones, where an irregular mesh is needed. The approach of modeling the Printed Circuit Boards (PCB) was the globally smeared technique, where the electronic components are not explicitly represented, but their total mass is taking into account with a uniform Non Structural Mass (NSM) parameter for each PCB. The model is compliant with the requirements related to the element geometry (skew, taper, aspect ratio, warp), damping definition (modal damping) and other modeling aspects specified in the Solar Orbiter project.

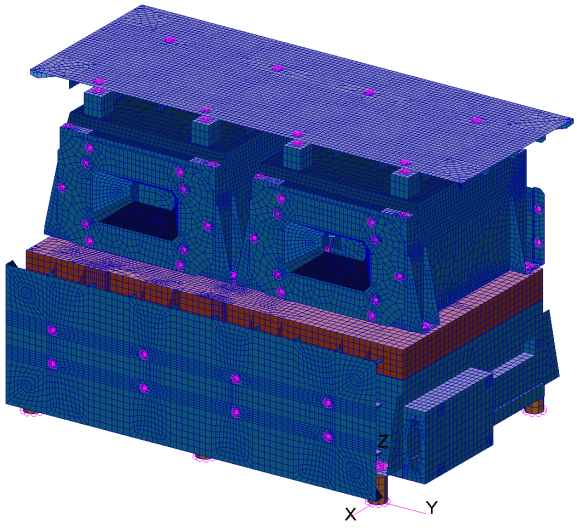

Figure 2-8: FEM of STEP instrument. The parts in blue are made of aluminum alloy EN AW 6061-T6 and the red part corresponds to the titanium (Ti 6Al 4V) cover

The structural parts of the instrument are made of aluminum alloy EN AW 6061-T6 and titanium alloy Ti 6Al 4V. Other materials included in the model are polyimide, copper and Ultem. The material properties are shown in Table 2-1.

Table 2-1: Material properties of STEP instrument

Material	Density (kg/m^3)	Young's modulus (GPa)	Poisson ratio
EN AW 6061-T6	2710	68.9	0.330
Ti 6Al 4V	4430	113.8	0.342
Polyimide	1850	24.8	0.180
Copper	8960	110.0	0.340
Ultem	1270	3.2	0.300

The main natural frequencies of the FEM are correlated with the low sine vibration test results until 2000 Hz. The main modes (with modal effective mass fractions greater than 10%) are within 400 and 1000 Hz (Table 2-2).

Table 2-2: First natural frequencies and modal effective masses for each axis obtained from FEM analysis

Natural frequency (Hz)	MEM (%) X axis	MEM (%) Y axis	MEM (%) Z axis	Frequency ratio (f_i/f_{i-1})
440.1	63.47	0.25	0.00	
551.6	0.51	37.61	2.00	1.253
553.0	0.06	25.46	8.73	1.003
632.1	0.14	0.23	0.00	1.143
638.8	0.38	0.00	0.00	1.011
658.9	0.00	0.06	0.11	1.031
668.4	0.29	0.33	0.02	1.014
685.8	0.98	0.00	0.09	1.026
755.1	0.02	1.14	28.90	1.101
781.1	0.16	1.30	4.09	1.034
809.9	0.11	12.96	3.79	1.037
833.5	1.26	0.00	1.73	1.029
912.6	0.00	0.00	0.08	1.095
931.5	0.02	0.27	3.47	1.021
977.3	0.25	9.25	2.60	1.049
990.5	0.03	2.67	10.58	1.013

With the purpose of employing the same FEM for shock analyses, it is important to check if it meets with the recommendations indicated by the European Space Agency (ESA) in [4].

The first recommendation is about the maximum length of the elements, which should be 8 times shorter than the flexural wavelength in thin-walled structures. In this instrument, the main parts are made of aluminum and titanium alloys with a minimum thickness of 1 mm. Using Eq. (1) [4] and considering the maximum frequency of 10000 Hz for shock analysis, the minimum wavelength is approximately 30 mm for both materials. This implies that the maximum recommended length for 2D elements is 3.75 mm, which is met in this instrument, where the maximum element length is 3 mm.

$$\lambda = \left(\frac{2\pi}{f}\right)^{1/2} \left(\frac{Et^2}{12\rho\left(1-\nu^2\right)}\right)^{1/4} \tag{1}$$

The time step for transient analysis is chosen based on the sampling rate of shock input signal, which is recommended to be at least 5 to 10 times higher than the maximum frequency of the analysis for implicit methods like Nastran. In this case, the shock load is specified until 10000 Hz, which gives an adequate value of 100000 Hz of sampling rate and a time step for analysis of 0.00001 s. This requirement is not as restrictive as for explicit codes, where the time step is of the order of magnitude of μs to get the numerical stability [4].

Another important recommendation indicated in [4] is that the mesh should be as homogeneous as possible. For 2D mesh, the preferred element shape is quadrilateral with one node per vertex (QUAD4), which is the predominant element type for STEP FEM. TRIA3 elements are used in some mesh transitions and represent the 5.5 % of the total of 2D elements.

With respect to the representation of non-structural parts, it is recommended for shock analysis to avoid the utilization of lumped masses attached with rigid elements, which can cause erroneous results in the adjacent elements. A recommended alternative is to increase the Non-Structural Mass (NSM) parameter for the zones where these non-structural parts are joined. In the FEM of STEP instrument, this approach has been employed for the mass representation of the electronic components for each electronic board.

3 Shock analysis methods

In this section, a summary of different FEM analysis options to simulate shock loads is presented considering the requirements and limitations indicated in the previous section for shock modeling and analysis in space projects. All proposed methods are compatible with Nastran code and linear analysis.

3.1 Transient analysis

Transient analysis is the most general way to compute the behavior of a structure subjected to a time-varying load or forced transient acceleration. Two transient methods are available in Nastran code: Modal Transient Response Analysis (Sol 112) and Direct Transient Response Analysis (Sol 109).

The main advantage of the both transient methods is the possibility to obtain time functions of any requested result (stresses, forces, accelerations). From these time functions, it is straightforward to calculate other forms to present the results used for shock evaluation as the peak values and the SRS curves. Therefore, the complete behavior of the analyzed structure can be obtained, but with the disadvantage of the high computational time and large amount of the results, which can exceed the capability of the computers in some cases. The requirement of using the modal damping formulation for STEP instrument analyses is incompatible with Direct Transient Response Analysis, where only viscous damping is allowed. For this reason, the transient analysis included in this study corresponds only to Modal Transient Response Analysis.

Simpler but less accurate alternative methods are summarized below with the advantage of being less time-consuming and of generating smaller amount of results.

3.2 Response Spectrum Analysis

The Response Spectrum Analysis (RSA) method consists in estimating directly the approximation of the peak responses of any type of result using a normal modes calculation of

the structure (Sol 103) and defining as input the SRS specification applied to the base. This method gives the typical results of normal modes calculation (list of natural frequencies in the range of interest, modal participation factors for each mode, etc.) and the peak values of the requested results. These peak values are obtained from the combination of all the modal contributions of acceleration. Thus, a modal combination method must be selected in the analysis from the following available options in Nastran:

- ABS: This summation method gives the most conservative results (high values of accelerations, forces and stresses) and consists in considering that all modal peak values of acceleration for every node occur in the same instant and phase. The total peak acceleration is the summation of the absolute values of each modal contribution.
- SRSS: The Square Root of the Summation of Squared values (SRSS) method gives the total peak acceleration in a similar way as assuming that the modal contributions are combined randomly, i.e. that the peak accelerations of each mode appear at different instants and phases. This approach is the most optimistic.
- NRL: This combinatory method was developed by the Naval Research Laboratories (NRL) as a compromise between the two previous options, and considers that for each excitation there is only one important mode that contributes the most into the peak response. Therefore, the total peak value is the sum of the absolute peak response associated to this mode and the SRSS calculation of the contribution of rest of modes. The results are in between than the two previous methods.
- CQC: The Complete Quadratic Combination (CQC) method involves the calculation of the cross-modal (covariance) coefficients for pairs of modes (p_{ij}) to take into account the coupling between these modes in the SRSS formulation.

The SRSS and NRL options provide the possibility of defining that consecutive modes with frequencies ratios below the threshold indicated by the parameter CLOSE are summed with ABS option, while the rest of modes are taking into account with SRSS or NRL methods respectively.

The main disadvantage of RSA method is the low accuracy of the results and the dependence with the chosen summation option.

3.3 Sine Transmissibility Method

An alternative method [4] to calculate SRS curves of response acceleration for selected nodes consists in multiplying the input SRS by the shock transmissibility (TF_i^{SHOCK}) between the base and the nodes of interest. The shock transmissibility can be estimated from the sine transmissibility using Eq. (2), where the parameter K can take a value between 1 and 2:

$$TF_i^{SHOCK} = \sqrt{K \cdot FRF_i^{SINE}} \tag{2}$$

The sine transmissibility can be calculated by a Frequency Response Analysis (Sol 111) or from the sine sweep test data. The main disadvantage of this method is that it cannot calculate the peak values neither the time functions of the response. Another inconvenience is the appreciable difference between the SRS curves calculated by this method and the SRS curves from tests results of this instrument, especially due to high peaks that appear in the natural frequencies when low damping value are considered.

3.4 Equivalent Quasi-Static Load Method

Finally, the last analysis method presented in this paper is the calculation of the equivalent quasi-static (EQS) inertial acceleration, which approximately gives the same total interface force as the shock load. Two different equations [4] are proposed depending on the modal coupling of the analyzed structure: Eq. (3) for decoupled main modes and Eq. (4) for coupled main modes.

$$\gamma_{EQS} = \frac{\sum_i \left[MEM_i x SRS(f_i) \right] + M_{Res} x SRS^{High\_frequency}}{M_{Total}} \tag{3}$$

$$\gamma_{EQS} = \frac{\sqrt{\sum_i \left[MEM_i x SRS(f_i) \right]^2 + \left[M_{Res} x SRS^{High\_frequency} \right]^2}}{M_{Total}} \tag{4}$$

The interface forces obtained from the static analysis (Sol 101) by applying the equivalent static acceleration correspond to the peak interface forces for the shock simulation.

4 FEM analysis results

The results (accelerations, forces and stresses) obtained to evaluate the STEP instrument subjected to the shock loads considering the proposed analysis methods are compared in different formats (peak values, time functions and SRS curves) to estimate their differences. In section 4.1, the input acceleration measured in the shock test (time acceleration functions or the corresponding SRS, depending of the analysis method) is simulated to compare the numerical results with the test data with the aim to determine the precision of each method. In section 4.2, the main results from the FEM analysis methods are compared to study their differences with the same SRS specification. For RSA and EQS methods, the SRS specification is applied directly. For the transient analysis, various time acceleration functions are calculated from the SRS specification and are applied as input with the objective to demonstrate the similarity between the results despite the differences on the input acceleration functions.

4.1 FEM analyses simulating the test environment

In this section, the peak values, transient signals and the corresponding SRS curves of acceleration of the points of the structure where the accelerometers were located in the shock test are calculated by the proposed analysis methods and are then compared with test results. For transient analyses, the input time signal measured by Ref2 accelerometer in Y direction (Figure 2-6) is applied as input. The effect on the results of including the cross input accelerations measured during shock test is also evaluated. For the rest of analysis methods, the SRS curve related to the measured signal in Y direction (Figure 2-4) by the Ref2 accelerometer is used as input. For the SRSS and NRL options, 4 values of the close parameter are considered: 1.001, 1.005, 1.01 and 1.10. The peak values calculated for the transient analysis and RSA methods considering different options for modal contribution summation are compared in Table 4-1 with test results at accelerometers locations. The indicated values correspond to the Y component of acceleration. The modal damping used for all analyses is the standard value of 0.05 [4] in the frequency range of interest (100 – 10000 Hz). The differences with respect to the acceleration peak values measured during the shock test in dB are in Table 4-2.

Table 4-1: Peak acceleration values (g) from different analysis methods for shock test simulation in Y direction

Type of analysis	Peak acceleration (g) at accelerometers locations					
	TriA2y	TriA3y	TriA4y	TriA5y	TriA6y	TriA7y
Test	207.49	359.49	180.84	186.48	180.25	402.99
Transient Analysis	228.95	268.00	189.77	191.73	225.62	269.78
RSA ABS	498.76	572.93	325.45	348.45	429.27	894.17
RSA SRSS	130.34	188.02	85.56	95.94	153.85	160.54
RSA SRSS close 1.001	157.43	220.32	107.59	115.78	169.12	245.36
RSA SRSS close 1.005	300.97	381.48	183.37	190.65	273.91	507.02
RSA SRSS close 1.01	355.29	452.31	224.93	235.94	293.62	693.26
RSA SRSS close 1.10	494.02	569.72	322.62	345.38	425.67	892.89
RSA NRL	181.23	264.14	118.70	133.58	216.11	222.63
RSA NRL close 1.001	208.29	296.28	140.54	153.29	231.31	305.93
RSA NRL close 1.005	349.88	451.93	215.47	226.94	331.24	565.16
RSA NRL close 1.01	403.49	520.30	256.10	271.15	350.89	743.89
RSA NRL close 1.10	498.08	571.51	325.28	348.17	428.21	893.65
RSA CQC	187.03	232.11	133.45	147.07	192.79	251.21

Table 4-2: Differences of peak acceleration values for different analysis methods with respect to test results

Type of analysis	Differences of Peak acceleration values (dB)					
	TriA2y	TriA3y	TriA4y	TriA5y	TriA6y	TriA7y
Transient Analysis	0.86	-2.55	0.42	0.24	1.95	-3.49
RSA ABS	7.62	4.05	5.10	5.43	7.54	6.92
RSA SRSS	-4.04	-5.63	-6.50	-5.77	-1.38	-7.99
RSA SRSS close 1.001	-2.40	-4.25	-4.51	-4.14	-0.55	-4.31
RSA SRSS close 1.005	3.23	0.52	0.12	0.19	3.63	1.99
RSA SRSS close 1.01	4.67	2.00	1.89	2.04	4.24	4.71
RSA SRSS close 1.10	7.53	4.00	5.03	5.35	7.46	6.91
RSA NRL	-1.18	-2.68	-3.66	-2.90	1.58	-5.15
RSA NRL close 1.001	0.03	-1.68	-2.19	-1.70	2.17	-2.39
RSA NRL close 1.005	4.54	1.99	1.52	1.71	5.29	2.94
RSA NRL close 1.01	5.78	3.21	3.02	3.25	5.79	5.32
RSA NRL close 1.10	7.61	4.03	5.10	5.42	7.52	6.92
RSA CQC	-0.90	-3.80	-2.64	-2.06	0.58	-4.11

The results indicate that the analysis method with smaller average error is the transient analysis, where the differences are below the limits of ±3 dB, except for TriA7y peak acceleration, where the difference is due to high frequency waves detected in the shock test, which cannot be obtained with accuracy from the FEM analysis. This discrepancy is discussed below, after the calculation and comparison of the SRS curves. Among the proposed options for RSA method, the most similar to test results correspond to the SRSS and NRL, both with CLOSE parameter of 1.001. But in general, this method presents high differences and variability which depend on the combination option with differences that oscillates between -8 dB and +8 dB approximately with respect to test results, where the most conservative is the ABS option and the most optimistic is the SRSS option.

The SRS curves of acceleration can be calculated with the modal transient analysis and with sine transmissibility approach. For this last method, Eq. (2) with $K = 1$ is applied to estimate the shock transmissibility from the sine transmissibility obtained from both sine sweep test and frequency response analysis. The modal damping of 0.05 for all frequency range is defined for

the transient and the frequency response analyses. To compute the SRS curves from the time functions of acceleration for the transient analysis and shock test results, the standard damping constant of 0.05 is used for all results presented in this paper. This damping parameter for SRS calculation has a different meaning and is independent of the damping factor defined in FEM analyses. The comparison of SRS curves obtained from these methods with the SRS curves from shock test is shown in Figure 4-1. The locations where the accelerometers of the shock test coincide with the accelerometers of the sine sweep test are TriA2y, TriA3y, TriA5y and TriA7y.

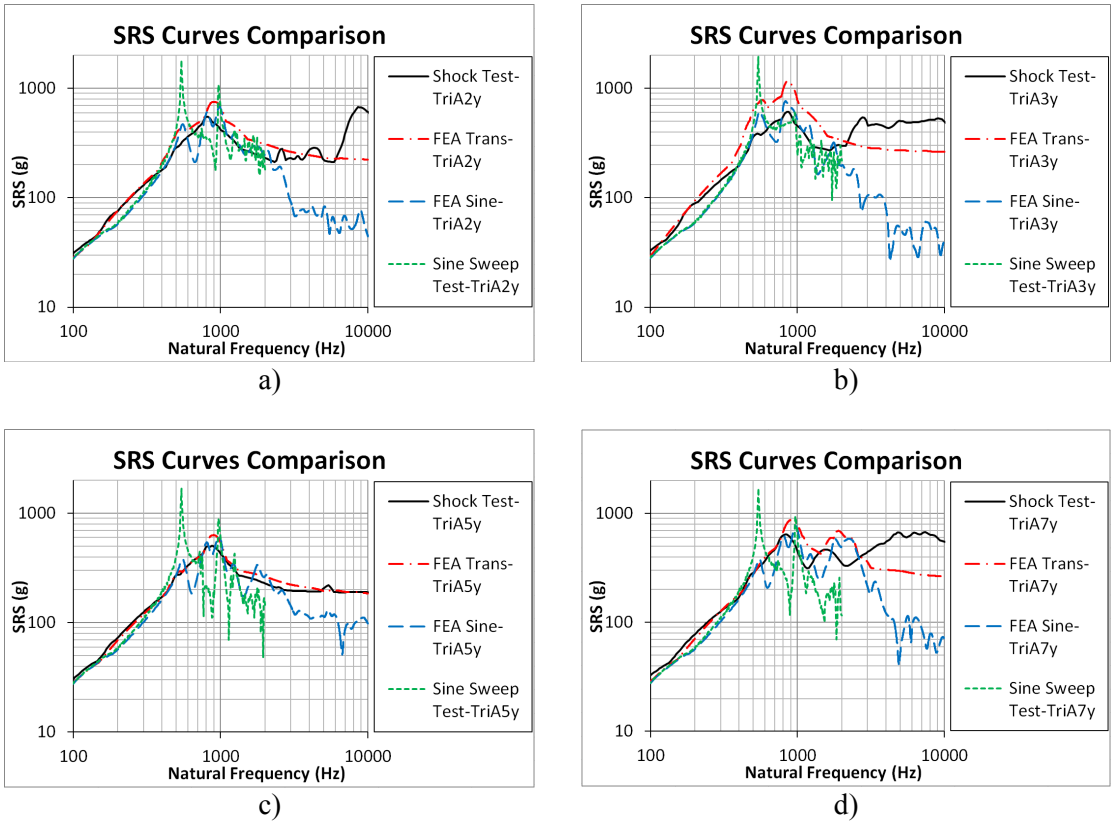

Figure 4-1: SRS curves for TriA2y (a), TriA3y (b), TriA5y (c) and TriA7y (d) accelerometers for shock test, transient analysis and sine transmissibility method with frequency response analysis and with sine sweep test results

The first conclusion is that transient analysis provides an acceptable prediction of the shock test results until 2000 Hz, which is the frequency range that contains the main natural frequencies of STEP instrument. But this analysis underestimates the response for the higher frequency range. These discrepancies are due to the generation of high frequency waves during the shock test, which appear at the end of the first loop of the main wave, as can be better appreciated in the comparison between time functions (Figure 4-3). The causes of these high frequency waves during test are unknown, but are not due to the input neither to any malfunction of the measuring equipment. The SRS curves calculated by the sine transmissibilities obtained from low sine test cover only up to 2000 Hz. The SRS curves obtained with this method present very high peaks and deep valleys due to that the damping factors for sine vibration are lower than for the shock test, resulting in too sharp SRS curves. The SRS curves obtained from the sine transmissibilities calculated with frequency response analysis and with a modal damping value of 0.05 are smoother than the previous SRS curves, but from 2000 Hz decay considerably. The explanation is that these SRS curves have the same trend as the sine transmissibility, which decreases to zero for frequencies higher than the natural frequencies of the system, unlike the SRS curves computed from time functions, which tend asymptotically to the peak value of the

functions for frequencies higher than the maximum frequency content of the signal. For this reason, the end section of the SRS curves computed by sine transmissibility method presents high differences with respect to the shock test results. A way to correct this defect consists in substituting this end section by a constant SRS line, as similar as proposed in [4].

4.1.1 Influence of considering the cross input excitation for transient analysis

A comparison of the results of the transient analysis considering the excitation only in the main axis (Y axis) measured in the test (Figure 2-6) and an excitation that combines the input signal in the 3 orthogonal axes (Figure 2-5, Figure 2-6 and Figure 2-7) is shown in Figure 4-2, using the modal damping factor of 0.05 for the analyses. Slight differences are observed in the Y component of the acceleration results, concluding that the influence of the cross input accelerations for these results is negligible in this instrument.

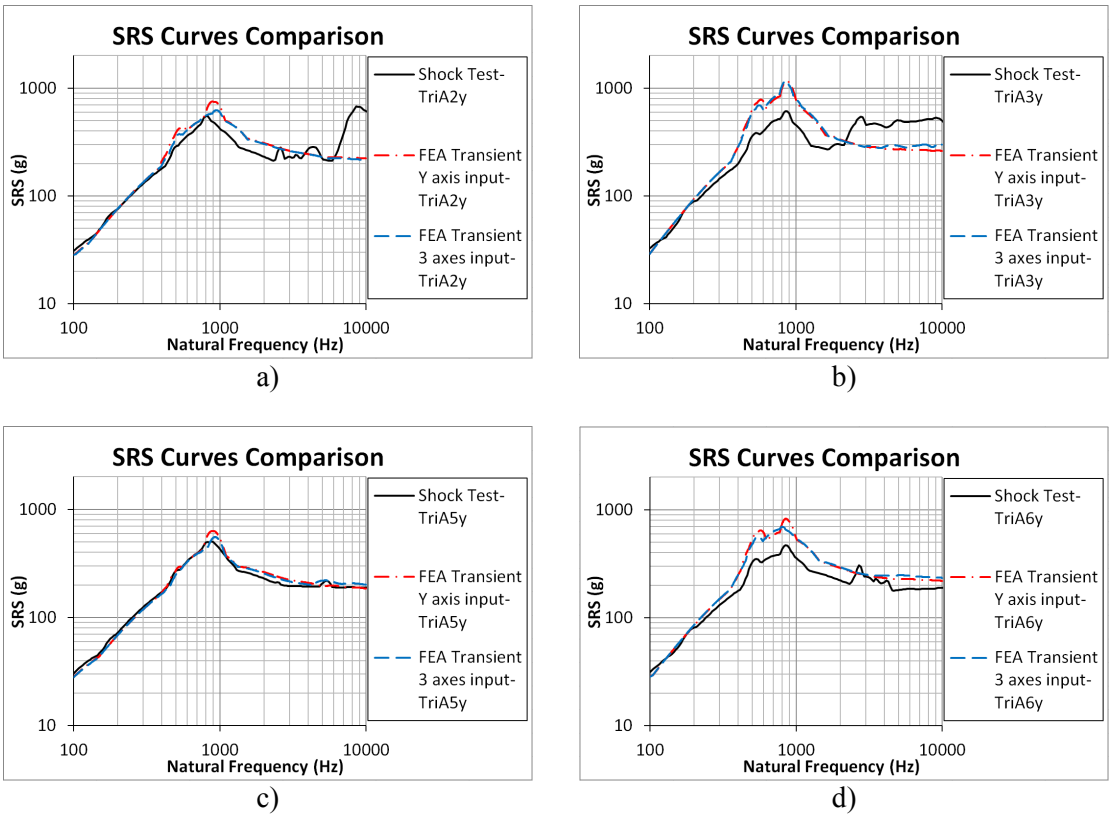

Figure 4-2: Comparison of SRS curves calculated by transient analysis between applying an excitation in the main axis and an excitation in the 3 orthogonal axes simultaneously

4.1.2 Influence of damping value for transient analysis

In this section, the influence of the damping value used for the transient analysis on the results is evaluated. Three different values are proposed (0.01, 0.05 and 0.15), each one is constant for all frequency range. The damping factor used to compute the SRS curves from the time functions is 0.05 for all of the results. As can be observed in Figure 4-3, the higher the damping used in the transient analysis the lower the acceleration peaks in time functions. The damping affects mainly in the frequency range where the natural frequencies are located (400 – 2000 Hz). When the damping value increases the SRS curves decrease and the peaks in the natural frequencies are hidden. The damping of 0.15 provides the SRS curves more similar to the test results for low and medium frequency bands, getting a very good correlation with the shock tests results measured by some accelerometers like TriA5y and TriA6y. However, a damping value of 0.01 for the high frequency range seems to be more adequate to correlate the response measured by TriA3y accelerometer.

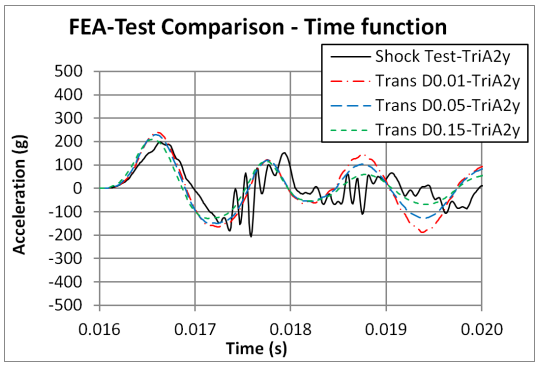

a)

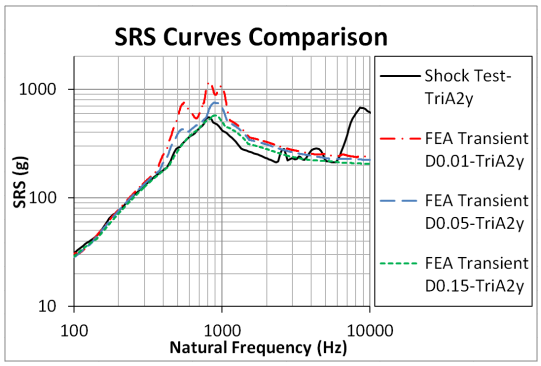

b)

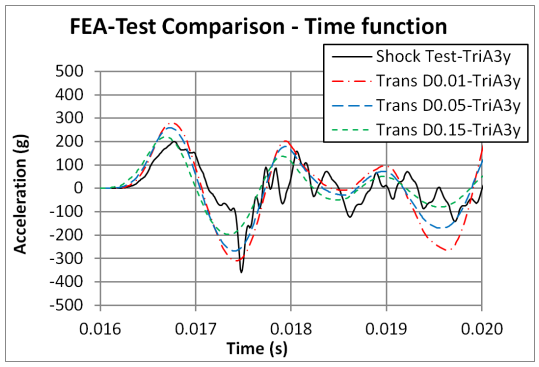

c)

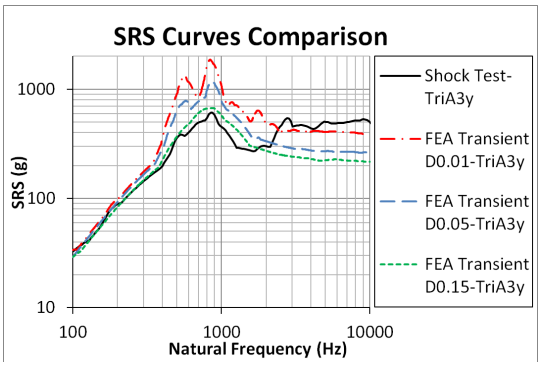

d)

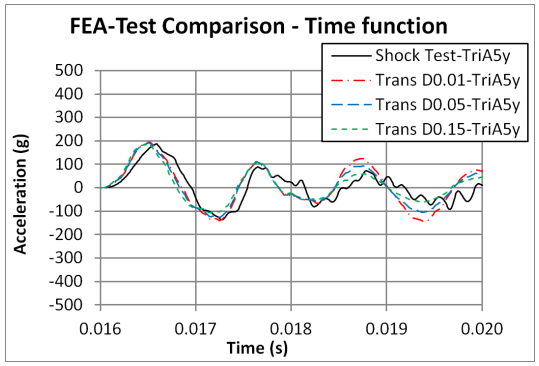

e)

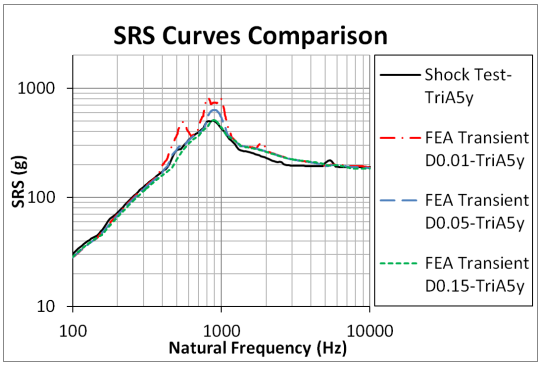

f)

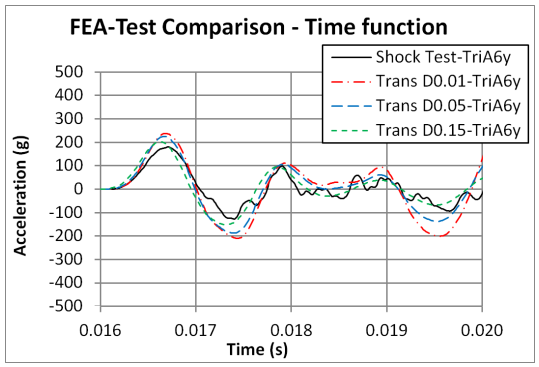

g)

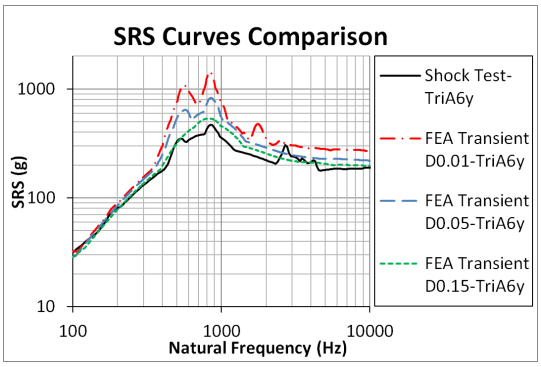

h)

Figure 4-3: Time functions and SRS curves of acceleration calculated by transient analysis for different values of damping: 0.01, 0.05 and 0.15

4.2 Comparison of FEA results using the SRS specification for STEP shock qualification

In this section, the shock environment is specified by a SRS curve instead of a transient acceleration function. This is the usual way to specify the shock environment for the majority of the space structures. For the transient analysis, the calculation of a transient acceleration function that meets with the specified SRS to be used as input in the analysis is needed as a previous step. For RSA method, the SRS is used directly as input. For EQS method, the input SRS is used to calculate the equivalent static acceleration.

4.2.1 Different input time functions from the SRS specification for transient analysis

To perform a transient analysis that simulates a shock environment specified by a SRS curve, it is necessary to have an input time acceleration function that meets the SRS specification. The drawback is that infinite options are possible, and therefore, one of the objectives of this study is to find out if the results (peak values and SRS curves) in transient analyses are similar considering different input functions from the same SRS.

Among different numerical calculations to obtain a time function from a given SRS, the most used methods are the damped sinusoids decomposition and the wavelet synthesis [4,5], because they give oscillatory acceleration functions that match the specified SRS with acceptable accuracy (Figure 4-4). One of the parameters that define the time functions is the duration. In order to evaluate its influence on the results, three different durations of 20, 40 and 100 ms have been proposed for both methods (Figure 4-5). In addition, a rectangular pulse (Figure 4-6) has been considered for the comparison, optimizing its two parameters (amplitude and duration) to better match the specified SRS, resulting in a rectangular pulse of 268.46 g and 0.2 ms.

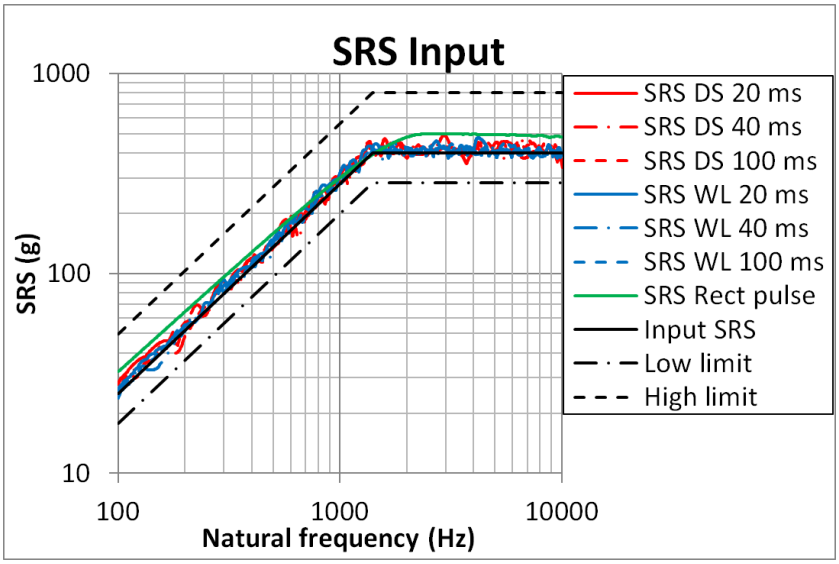

Figure 4-4: SRS curves for different input time acceleration functions: oscillatory functions obtained by damped sinusoids decomposition (DS) and by wavelet synthesis (WL) for three different signal durations (20, 40 and 100 ms) and a rectangular pulse of 268.46g and 0.2 ms

In Table 4-3 the absolute peak values of acceleration and the durations of the proposed input time functions are summarized.

Table 4-3: Maximum peak values and durations for input time acceleration functions for transient analyses

Input	Maximum peak acceleration (g)	Duration of signal (ms)
Damped sinusoids DS 20 ms	217	20
Damped sinusoids DS 40 ms	176	40
Damped sinusoids DS 100 ms	149	100
Wavelet synthesis WL 20 ms	196	20
Wavelet synthesis WL 40 ms	189	40
Wavelet synthesis WL 100 ms	152	100
Rectangular pulse	268	0.2

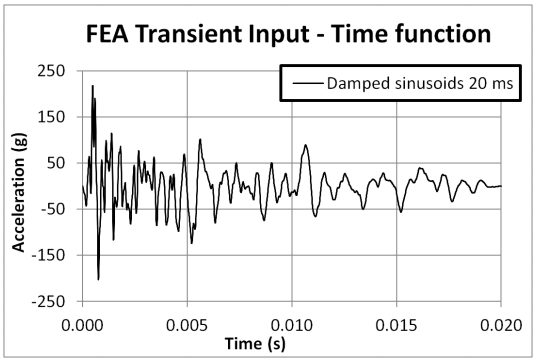

a) DS 20 ms

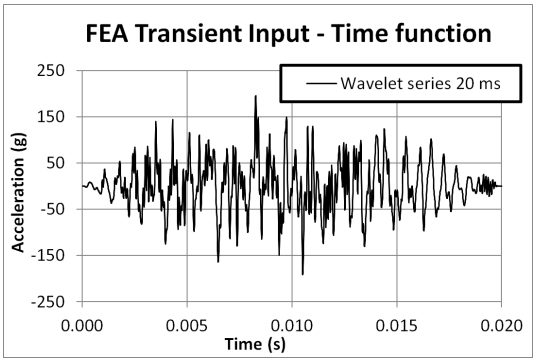

b) WL 20 ms

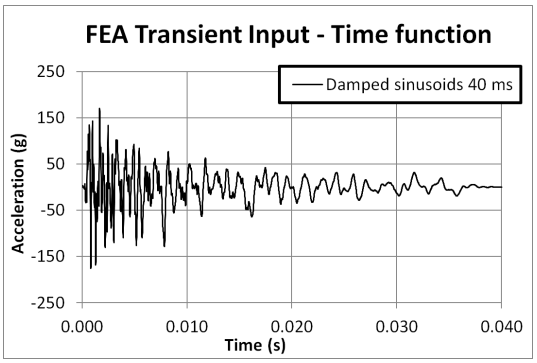

c) DS 40 ms

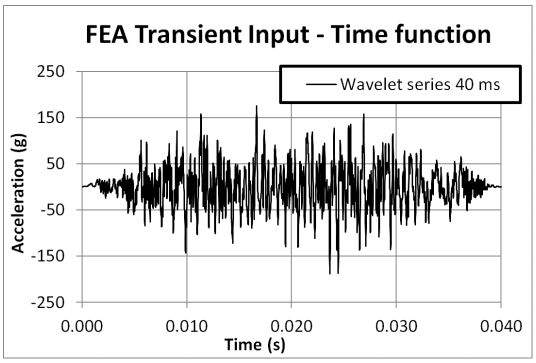

d) WL 40 ms

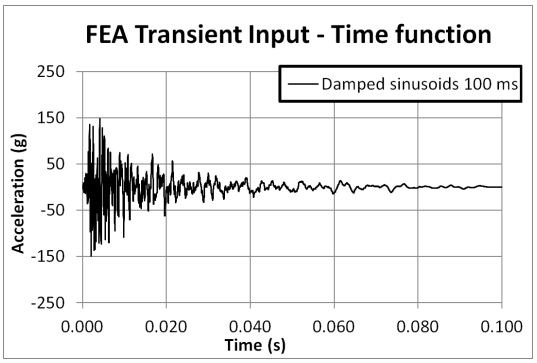

e) DS 100 ms

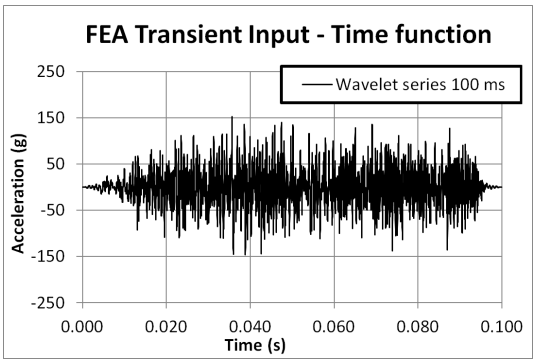

f) WL 100 ms

Figure 4-5: Input time functions of acceleration for transient analyses obtained by damped sinusoids summation method (left) and by wavelet synthesis (right)

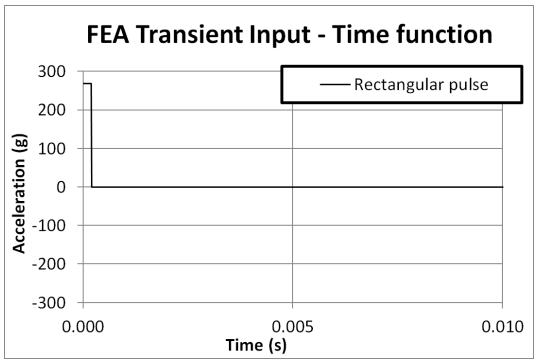

Figure 4-6: Rectangular pulse of 268.46g and 0.2 ms for input time function of acceleration for transient analysis

4.2.2 Comparison of peak results for different numerical shock analyses

The results which typically are calculated to evaluate the structural behavior of a space instrument are the maximum stresses, interface forces and accelerations. For the shock analyses, the maximum absolute values for these magnitudes, i.e. the peak values, are used to evaluate the structure. In this section, a comparison of these results for different analysis methods is established. The modal damping factor for all analyses corresponds to the standard value of 0.05 for the shock. For the transient analyses, seven different acceleration time functions (Figure 4-5 and Figure 4-6) are applied as input. For RSA method, different modal summation options are applied (ABS, SRSS, NRL and CQC), and with values of 1.001, 1.005, 1.01 and 1.10 for the CLOSE parameter for the options SRSS and NRL. For the calculation of interface forces, the EQS method is included in the comparison, considering the options for coupled and decoupled normal modes. The peak values of acceleration calculated by the proposed set of numerical analyses are shown in Table 4-4. With the aim to provide the differences, the transient analysis with an input of 20 ms has been chosen as reference case because this input load is the most similar to the input test environment (Figure 2-6). The differences of the results of the rest of methods with the reference case are indicated in Table 4-5.

Table 4-4: Peak values of acceleration calculated by different numerical analysis

Type of analysis	Peak acceleration (g) at accelerometers locations					
	TriA2y	TriA3y	TriA4y	TriA5y	TriA6y	TriA7y
Transient DS 20 ms	145.11	159.51	131.98	125.25	143.67	215.77
Transient DS 40 ms	175.87	206.61	143.87	148.41	174.01	300.77
Transient DS 100 ms	125.31	181.39	99.66	100.48	151.35	228.20
Transient WL 20 ms	143.39	200.80	125.75	120.48	152.36	268.80
Transient WL 40 ms	140.46	207.81	97.40	105.47	161.25	258.31
Transient WL 100 ms	143.35	178.27	113.15	115.36	153.14	266.03
Transient Rect pulse	257.76	265.31	221.04	220.48	227.95	394.30
RSA ABS	442.23	501.42	282.56	297.06	344.83	946.94
RSA SRSS	90.02	134.31	59.85	67.31	107.17	147.38
RSA SRSS close 1.001	122.37	171.21	83.90	89.15	123.95	243.03
RSA SRSS close 1.005	276.42	335.56	163.50	165.92	224.74	543.00
RSA SRSS close 1.01	339.86	412.50	209.64	216.30	249.06	765.94
RSA SRSS close 1.10	439.31	499.15	280.86	295.20	342.47	946.07
RSA NRL	125.09	189.46	80.08	91.25	151.51	198.78
RSA NRL close 1.001	157.40	226.09	103.99	112.95	168.14	293.33
RSA NRL close 1.005	309.58	384.48	183.10	189.00	262.45	591.54
RSA NRL close 1.01	371.44	456.45	228.16	237.93	286.57	798.51
RSA NRL close 1.10	441.71	500.34	282.43	296.84	344.06	946.56
RSA CQC	113.73	170.24	77.02	86.35	136.49	192.42

Table 4-5: Differences between peak values of acceleration calculated by different numerical analyses

Type of analysis	Differences for peak acceleration values (dB)					
	TriA2y	TriA3y	TriA4y	TriA5y	TriA6y	TriA7y
Transient DS 40 ms	1.67	2.25	0.75	1.47	1.66	2.88
Transient DS 100 ms	-1.27	1.12	-2.44	-1.91	0.45	0.49
Transient WL 20 ms	-0.10	2.00	-0.42	-0.34	0.51	1.91
Transient WL 40 ms	-0.28	2.30	-2.64	-1.49	1.00	1.56
Transient WL 100 ms	-0.11	0.97	-1.34	-0.71	0.55	1.82
Transient Rect pulse	4.99	4.42	4.48	4.91	4.01	5.24
RSA ABS	9.68	9.95	6.61	7.50	7.60	12.85
RSA SRSS	-4.15	-1.49	-6.87	-5.39	-2.55	-3.31
RSA SRSS close 1.001	-1.48	0.61	-3.94	-2.95	-1.28	1.03
RSA SRSS close 1.005	5.60	6.46	1.86	2.44	3.89	8.02
RSA SRSS close 1.01	7.39	8.25	4.02	4.75	4.78	11.00
RSA SRSS close 1.10	9.62	9.91	6.56	7.45	7.55	12.84
RSA NRL	-1.29	1.49	-4.34	-2.75	0.46	-0.71
RSA NRL close 1.001	0.71	3.03	-2.07	-0.90	1.37	2.67
RSA NRL close 1.005	6.58	7.64	2.84	3.57	5.23	8.76
RSA NRL close 1.01	8.16	9.13	4.75	5.57	6.00	11.37
RSA NRL close 1.10	9.67	9.93	6.61	7.50	7.59	12.84
RSA CQC	-2.12	0.57	-4.68	-3.23	-0.45	-1.00

The differences between the peak values calculated by the transient analyses with the proposed inputs are within the limits of ±3 dB, except for the input rectangular pulse, which shows higher peak values. The dispersion of results calculated by all the options for RSA method are high, with differences out of the range of ±3 dB, being the NRL option with CLOSE parameter of 1.001 the most similar to transient analyses.

The forces calculated for each interface bolt (IF1 – IF6) of STEP instrument are shown in Table 4-6. The differences between results with respect to the reference case (transient analysis with 20 ms of acceleration input) are shown in Table 4-7. Similar to the acceleration results, the differences between the transient analyses results are within the limits of ±3 dB. The NRL option for RSA method gets the results more similar to those of transient analyses. The results of EQS method for decoupled modes and coupled modes are quite similar to that for RSA ABS option and RSA SRSS option respectively.

Table 4-6: Peak values of interface lateral forces calculated by different numerical analyses

Type of analysis	Lateral peak force for interface bolts (N)					
	IF1	IF2	IF3	IF4	IF5	IF6
Transient DS 20 ms	331	311	316	320	306	321
Transient DS 40 ms	426	405	420	384	378	385
Transient DS 100 ms	319	302	312	310	296	308
Transient WL 20 ms	301	280	291	307	284	307
Transient WL 40 ms	329	307	307	310	295	307
Transient WL 100 ms	324	308	315	315	303	315
Transient Rect pulse	531	504	522	467	462	465
RSA ABS	576	545	565	530	518	533
RSA SRSS	235	219	225	223	212	225
RSA SRSS 1.001	247	229	239	231	220	233
RSA SRSS 1.005	354	326	339	335	318	338
RSA SRSS 1.01	386	359	371	372	356	379
RSA SRSS 1.10	567	535	552	523	511	526
RSA NRL	331	309	318	315	299	317
RSA NRL 1.001	344	319	332	323	307	325
RSA NRL 1.005	440	406	422	404	389	408
RSA NRL 1.01	470	438	453	439	425	447
RSA NRL 1.10	573	542	561	528	517	533
RSA CQC	301	281	289	301	283	301
EQS Decoupled Modes	557	530	550	538	518	536
EQS Coupled Modes	228	217	225	220	212	219

Table 4-7: Differences between peak values of interface lateral forces calculated by different numerical analyses

Type of analysis	Differences for peak force values (dB)					
	IF1	IF2	IF3	IF4	IF5	IF6
Transient DS 40 ms	2.18	2.30	2.47	1.59	1.84	1.58
Transient DS 100 ms	-0.34	-0.26	-0.11	-0.29	-0.28	-0.35
Transient WL 20 ms	-0.84	-0.89	-0.74	-0.35	-0.64	-0.38
Transient WL 40 ms	-0.06	-0.11	-0.25	-0.28	-0.31	-0.39
Transient WL 100 ms	-0.19	-0.07	-0.04	-0.13	-0.08	-0.17
Transient Rect pulse	4.09	4.21	4.35	3.27	3.58	3.22
RSA ABS	4.80	4.87	5.04	4.38	4.57	4.41
RSA SRSS	-3.00	-3.06	-2.94	-3.14	-3.20	-3.10
RSA SRSS 1.001	-2.55	-2.64	-2.44	-2.85	-2.87	-2.80
RSA SRSS 1.005	0.57	0.42	0.60	0.40	0.34	0.43
RSA SRSS 1.01	1.31	1.25	1.39	1.30	1.32	1.45
RSA SRSS 1.10	4.66	4.72	4.83	4.27	4.45	4.28
RSA NRL	-0.01	-0.06	0.05	-0.14	-0.19	-0.11
RSA NRL 1.001	0.31	0.23	0.41	0.07	0.04	0.10
RSA NRL 1.005	2.45	2.33	2.50	2.03	2.07	2.08
RSA NRL 1.01	3.04	2.99	3.13	2.75	2.85	2.88
RSA NRL 1.10	4.75	4.84	4.98	4.35	4.55	4.40
RSA CQC	-0.83	-0.86	-0.80	-0.53	-0.68	-0.57
EQS Decoupled Modes	4.51	4.65	4.80	4.50	4.57	4.45
EQS Coupled Modes	-3.24	-3.11	-2.95	-3.25	-3.19	-3.31

The most stressed part of STEP instrument is the titanium cover on top of the Ebox and below the detectors (Figure 2-8). The maximum peak stress values are compared in Table 4-8 and the peak stress distributions are shown in Figure 4-7 for transient analysis (input acceleration

function of 20 ms), in Figure 4-8 for RSA with ABS option and in Figure 4-9 for RSA with SRSS option. The stress distributions are very similar between the different methods, where the maximum stresses are located in the same zone. The biggest differences of the peak stress values correspond to RSA ABS (+5 dB) and to RSA SRSS (-4 dB). The RSA option with less difference with respect to transient analysis is SRSS option with a CLOSE threshold of 1.005.

Table 4-8: Maximum peak stress for titanium cover of STEP instrument calculated by different numerical analyses

Type of analysis	Maximum stress (MPa)	Difference (dB)
Transient DS 20 ms	89.2	-
RSA ABS	158.0	4.97
RSA SRSS	56.9	-3.91
RSA SRSS 1.001	60.4	-3.39
RSA SRSS 1.005	86.9	-0.23
RSA SRSS 1.01	101.0	1.08
RSA SRSS 1.10	146.0	4.28
RSA NRL	80.3	-0.91
RSA NRL 1.001	82.7	-0.66
RSA NRL 1.005	107.0	1.58
RSA NRL 1.01	118.0	2.43
RSA NRL 1.10	155.0	4.80
RSA CQC	76.2	-1.37

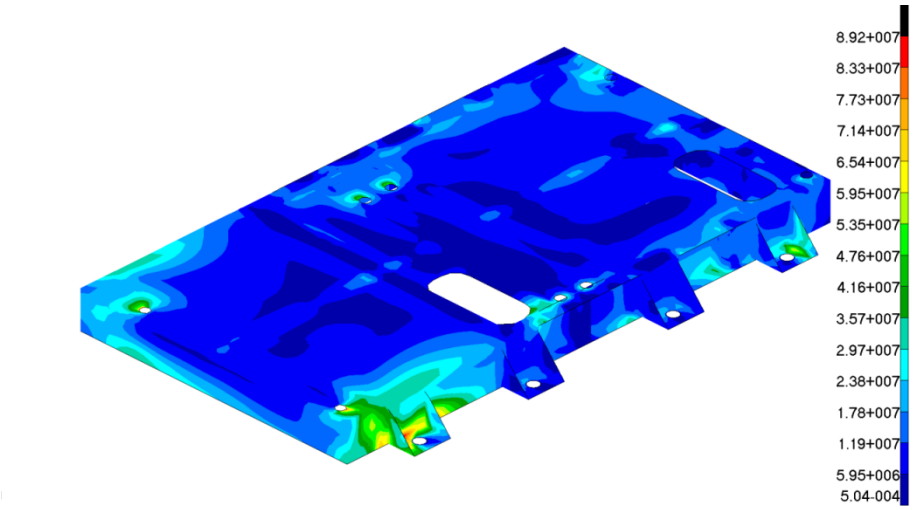

Figure 4-7: Stress distribution (Pa) on Titanium Cover calculated by transient analysis (DS 20 ms)

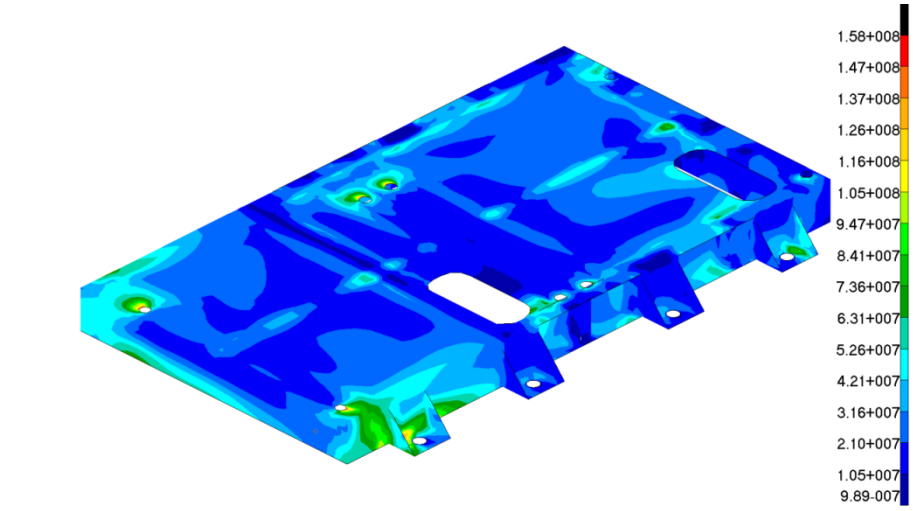

Figure 4-8: Stress distribution (Pa) on Titanium Cover calculated by RSA method with ABS option

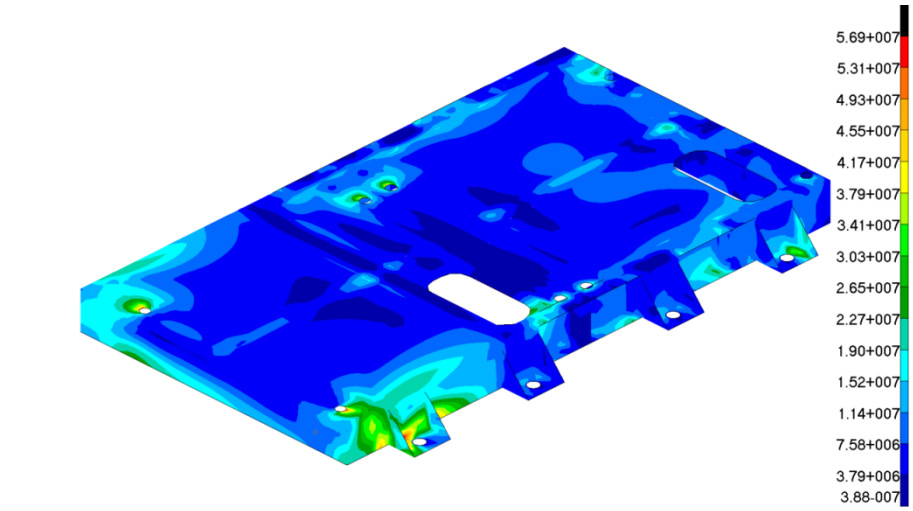

Figure 4-9: Stress distribution (Pa) on Titanium Cover calculated by RSA method with SRSS option

4.2.3 Comparison of SRS curves obtained from different input functions in transient analyses

The transient analyses using the different input acceleration functions give different response functions, but their corresponding SRS curves are quite similar among them as can be seen in Figure 4-10, with differences within ±3 dB, except for the rectangular pulse, with differences as much as +6 dB with respect to the other analyses.

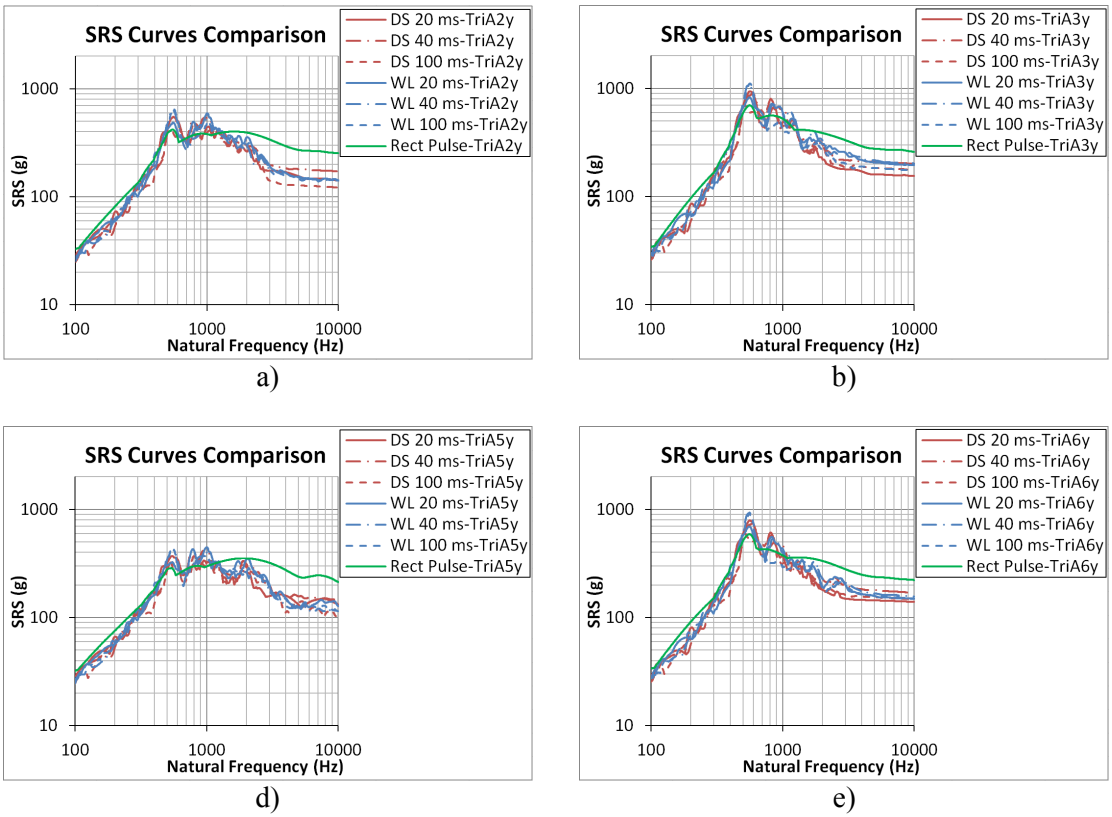

Figure 4-10: Comparison of response SRS curves calculated by transient analyses considering different acceleration inputs that match the specified SRS: oscillatory functions by damped sinusoids decomposition (DS), wavelet synthesis (WL) methods (with durations of 20, 40 and 100 ms) and with a rectangular pulse

5 Conclusions

This study has exposed an overview of the numerical analyses that can be employed to evaluate a space instrument subjected to the shock environment using the finite element model approach and taking into account the requirements imposed in space projects for structural analysis. A brief description of each method indicating the main advantages and disadvantages has been included and are summarized in Table 5-1. The modal transient analysis presents the best precision and is the only method capable of providing all the required results for structural verification in various formats as time functions, peak values and SRS curves. Its main disadvantage is the high computational cost in terms of analysis time and amount of output data. The differences of acceleration results with respect to the shock test measures are within the tolerable limits, except for TriA7y measure, where the difference is mainly due to the high frequency content of the test signals that cannot be reproduced with accuracy in the transient analysis. The rest of analysis methods present high dispersion of results and are quite dependent on the selected analysis option.

Table 5-1: Summary of studied shock analysis methods

Analysis method	Precision	Time of analysis and amount of output data	Type of results		
			Time functions	Peak values	Acceleration SRS curves
Modal transient	Good	High	X	X	X
RSA	Bad	Low		X	
Sine transmissibility	Medium	Low			X
EQS	Bad	Low		X*	

*Only for IF forces

This study has demonstrated that the transient analyses performed on a FEM of a small structure as the STEP instrument provide accurate simulations of the shock environment, having a greater confidence in the calculated results, which offer more information than the data obtained from shock test.

If it is not feasible to perform transient analysis due to its high computational cost or if a quick evaluation is needed, the rest of studied methods can be useful to evaluate the shock environment, but their lack of precision in some aspects and their limitations should be taken into account. For a conservative calculation of the response peak values, RSA with ABS option is the recommended analysis. This analysis can be performed together with SRSS option to know the maximum range of possible peak values for shock analyses. Intermediate options like CQC or NRL or by using an adequate value for CLOSE parameter with SRSS or NRL options provide more accurate results. An alternative to calculate in an easy way the peak values of the interface forces is the EQS method, where the results with decoupled normal modes formulation are as conservative as with RSA ABS option, while with coupled normal modes are similar as with RSA SRSS. If the calculation of response SRS curves is required to evaluate any critical component or to derive the SRS specification to an internal part, transient analysis is the recommended method because it provides accurate results, while with the sine transmissibility method the resulted SRS curves must be corrected in the high frequency range.

In the case where to qualify a space structure the shock environment is only specified in a SRS format, different possible time functions of acceleration can be used for transient analysis. This study has demonstrated that the differences of the results (peak values and response SRS curves) are within the tolerable limits considering a varied set of oscillatory functions determined by damped sinusoids decomposition and wavelet synthesis methods and a rectangular pulse that best match the specified SRS.

Acknowledgements

This work has been funded by the Spanish “Ministerio de Economía, Industria y Competitividad” through projects ESP2014-56169-C6-6-R and ESP2016-77548-C5-3-R. The authors wish to thank the team at Institute of Experimental and Applied Physics of the Christian Albrechts University of Kiel (IEAP-CAU) to give us the opportunity of working in this project and to supply the necessary data to make this study possible.

References

[1] M. Bellini, A. Calvi, Dynamic Analysis and loads definition for the structural design of the Euclid spacecraft, Proc. Int. Conf. Noise Vib. Eng. {ISMA 2014}. (2014) 809–820.

[2] A. Calvi, P. Bastia, Mechanical architecture and loads definition for the design and testing of the Euclid spacecraft, Adv. Aircr. Spacecr. Sci. 3 (2016) 225–242. doi:10.12989/aas.2016.3.2.225.

[3] J.-R. Lee, C.C. Chia, C.-W. Kong, Review of pyroshock wave measurement and simulation for space systems, Measurement. 45 (2012) 631–642. doi:10.1016/j.measurement.2011.12.011.

[4] ECSS, ECSS-E-HB-32-25A, Space engineering, Mechanical shock design and verification handbook, ESA-ESTEC Requirements and Standards Division, Noordwijk, 2015.

[5] J.J. Wijker, Spacecraft Structures, Springer Berlin Heidelberg, Berlin, Heidelberg, 2008. doi:10.1007/978-3-540-75553-1.

[6] R. Monti, P. Gasbarri, Dynamic load synthesis for shock numerical simulation in space structure design, Acta Astronaut. 137 (2017) 222–231. doi:10.1016/j.actaastro.2017.04.023.

[7] S. Mary, D. Dilhan, V. Cipolla, Shocks Environment Qualification of Demeter Microsatellite, in: K. Fletcher (Ed.), Proc. 5th Int. Symp. Environ. Test. Sp. Program., Noordwijk, 2004: pp. 555–562.

[8] A. Lacher, N. Jüngel, U. von Wagner, A. Bäger, Analytical calculation of in-plane response of plates with concentrated masses to impact and application to pyroshock simulation, J. Sound Vib. 331 (2012) 3358–3370. doi:10.1016/j.jsv.2012.02.024.

[9] A. Lacher, N. Jüngel, U. von Wagner, A. Bäger, Analytical prediction and optimization of far-field pyroshock test procedures, in: Eur. Sp. Agency, (Special Publ. ESA SP, 2012.

[10] O. Morais, C. Vasques, Shock environment design for space equipment testing, Proc. Inst. Mech. Eng. Part G J. Aerosp. Eng. 231 (2017) 1154–1167. doi:10.1177/0954410016648998.

[11] M. Sutra, D. Mesnier, A. Berlioz, B. Combes, Development of a simulation process of the behaviour of space equipment subjected to pyrotechnic shocks, based on characterization and environmental tests, Proc. Eur. Conf. Spacecr. Struct. Mater. Mech. Test. (2005) 243–247.

[12] S. Kiryenko, G. Piret, J. Kasper, ESA/ESTEC Shock Bench Presentation, in: Proc. Eur. Conf. Spacecr. Struct. Mater. Mech. Test. 2005 (ESA SP-581), 2005.

[13] R. Velmurugan, E. Mohamed Najeeb, Study of Far-Field Pyroshock Responses of Composite Panels, J. Vib. Acoust. 136 (2014) 31014. doi:10.1115/1.4027223.

[14] D. Wattiaux, O. Verlinden, C. Conti, C. De Fruytier, Prediction of the Vibration Levels Generated by Pyrotechnic Shocks Using an Approach by Equivalent Mechanical Shock, J. Vib. Acoust. 130 (2008) 41012. doi:10.1115/1.2827985.

[15] K. Karpanan, B. O'Toole, Experimental and Numerical Analysis of Structures With Bolted Joints Subjected to Low Impact Load: Part 1, in: Vol. 5 High-Pressure Technol. Rudy Scavuzzo Student Pap. Symp. 24th Annu. Student Pap. Compet. ASME Nondestruct. Eval. Diagnosis Progn. Div. (NDPD); Electr. Power Res. Inst. Creep Fatigue Work., ASME, 2016: p. V005T05A023. doi:10.1115/PVP2016-63711.

[16] Y.J. Mao, H.J. Huang, Y.X. Yan, Numerical Techniques for Predicting Pyroshock Responses of Aerospace Structures, Adv. Mater. Res. 108–111 (2010) 1043–1048. doi:10.4028/www.scientific.net/AMR.108-111.1043.

[17] S. Jayaraman, M. Trikha, Somashekar, D. Kamesh, M. Ravindra, Response Spectrum Analysis of Printed Circuit Boards Subjected to Shock Loads, Procedia Eng. 144 (2016) 1469–1476. doi:10.1016/j.proeng.2016.06.710.

[18] G. Parzianello, A. Francesconi, D. Pavarin, An estimation method for the Shock Response Spectrum propagating into plates subjected to hypervelocity impact, Measurement. 43 (2010) 92–102. doi:10.1016/j.measurement.2009.07.010.

[19] J. Thota, M.B. Trabia, B.J. O'Toole, Simulation of Shock Response in a Lab-Scale Space Frame Structure Using Finite Element Analysis, in: Vol. 7 Dyn. Syst. Control. Mechatronics Intell. Mach. Parts A B, ASME, Denver, 2011: pp. 725–731. doi:10.1115/IMECE2011-64353.

[20] M. de Benedetti, G. Garofalo, M. Zumpano, R. Barboni, On the damping effect due to bolted junctions in space structures subjected to pyro-shock, Acta Astronaut. 60 (2007) 947–956. doi:10.1016/j.actaastro.2006.11.011.

[21] Z.-Y. Qin, S.-Z. Yan, F.-L. Chu, Dynamic characteristics of launch vehicle and spacecraft connected by clamp band, J. Sound Vib. 330 (2011) 2161–2173. doi:10.1016/j.jsv.2010.06.011.

[22] D. Cui, S. Yan, J. Li, Z. Qin, X. Guo, Dynamic analysis of satellite separation considering the flexibility of interface rings, Proc. Inst. Mech. Eng. Part G J. Aerosp. Eng. 229 (2015) 1886–1902. doi:10.1177/0954410014562012.

[23] B.C. Ma, X.K. Tian, Simulation Analysis to Shock Strength of Electromechanical Products Using MSC.PATRAN and MSC.DYTRAN, Adv. Mater. Res. 201–203 (2011) 272–275. doi:10.4028/www.scientific.net/AMR.201-203.272.

[24] A.S. Ranouta, X. Fan, Q. Han, Shock performance study of solder joints in wafer level packages, in: 2009 Int. Conf. Electron. Packag. Technol. High Density Packag., IEEE, 2009: pp. 1266–1276. doi:10.1109/ICEPT.2009.5270604.

[25] H.-C. Cheng, T.-H. Cheng, W.-H. Chen, T.-C. Chang, H.-Y. Huang, Board-Level Drop Impact Reliability of Silicon Interposer-Based 2.5-D IC Integration, IEEE Trans. Components, Packag. Manuf. Technol. 6 (2016) 1493–1504. doi:10.1109/TCPMT.2016.2603192.

[26] J. Qiankun, D. Gangyi, A finite element analysis of ship sections subjected to underwater explosion, Int. J. Impact Eng. 38 (2011) 558–566. doi:10.1016/j.ijimpeng.2010.11.005.

[27] X. Wang, Z. Qin, J. Ding, F. Chu, Finite element modeling and pyroshock response analysis of separation nuts, Aerosp. Sci. Technol. 68 (2017) 380–390. doi:10.1016/j.ast.2017.05.028.

[28] A. Cicirello, R.S. Langley, T. Street, Modelling the shock induced failure of printed circuit boards, Proc. 9th Int. Conf. Struct. Dyn. EURODYN 2014. (2014) 3251–3258.

[29] D.-O. Lee, J.-H. Han, H.-W. Jang, S.-H. Woo, K.-W. Kim, Shock Response Prediction of a Low Altitude Earth Observation Satellite During Launch Vehicle Separation, Int. J. Aeronaut. Sp. Sci. 11 (2010) 49–57. doi:10.5139/IJASS.2010.11.1.049.

[30] M. Gherlone, D. Lomario, M. Mattone, R. Ruotolo, Application of Wave Propagation to Pyroshock Analysis, Shock Vib. 11 (2004) 145–156. doi:10.1155/2004/278676.

[31] R. Gómez-Herrero, J. Rodríguez-Pacheco, R.F. Wimmer-Schweingruber, G.M. Mason, S. Sánchez-Prieto, C. Martín, M. Prieto, G.C. Ho, F.E. Lara, I. Cernuda, J.J. Blanco, A. Russu, O.R. Polo, S.R. Kulkarni, C. Terasa, L. Panitzsch, S.I. Böttcher, S. Boden, B. Heber, J. Steinhagen, J. Tammen, J. Köhler, C. Drews, R. Elftmann, A. Ravanbakhsh, L. Seimetz, B. Schuster, M. Yedla, E. Valtonen, R. Vainio, The Solar Orbiter Mission: an Energetic Particle Perspective, (2017) 1–8. http://arxiv.org/abs/1701.04057.